Journal of Biomechanics 82 (2019) 124–133

Contents lists available at ScienceDirect

Journal of Biomechanics

journal homepage: www.elsevier.com/locate/jbiomech
www.JBiomech.com

Can altered neuromuscular coordination restore soft tissue loading patterns in anterior cruciate ligament and menisci deficient knees during walking? ☆

Colin R. Smith [a], Scott C.E. Brandon [a,b], Darryl G. Thelen [a,*]

[a] Department of Mechanical Engineering, University of Wisconsin-Madison, USA
[b] School of Engineering, University of Guelph, Canada

ARTICLE INFO

Article history:
Accepted 19 October 2018

Keywords:
Anterior cruciate ligament
Meniscus
Musculoskeletal modeling
Cartilage loading
Neuromuscular coordination

ABSTRACT

Injuries to the anterior cruciate ligament (ACL) and menisci commonly lead to early onset osteoarthritis. Treatments that can restore normative cartilage loading patterns may mitigate the risk of osteoarthritis, though it is unclear whether such a goal is achievable through conservative rehabilitation. We used musculoskeletal simulation to predict cartilage and ligament loading patterns during walking in intact, ACL deficient, menisci deficient, and ACL-menisci deficient knees. Stochastic simulations with varying coordination strategies were then used to test whether neuromuscular control could be modulated to restore normative knee mechanics in the pathologic conditions. During early stance, a 3 mm increase in anterior tibial translation was predicted in the ACL deficient knee. Mean cartilage contact pressure increased by 18% and 24% on the medial and lateral plateaus, respectively, in the menisci deficient knee. Variations in neuromuscular coordination were insufficient to restore normative cartilage contact patterns in either the ACL or menisci deficient knees. Elevated cartilage contact pressures in the pathologic knees were observed in regions where cartilage wear patterns have previously been reported. These results suggest that altered cartilage tissue loading during gait may contribute to region-specific degeneration patterns, and that varying neuromuscular coordination in isolation is unlikely to restore normative knee mechanics.

1. Introduction

Conservative treatment for anterior cruciate ligament (ACL) and menisci injuries enable patients to forego surgery. However, it is unclear whether rehabilitation alone can restore normative knee mechanics and thereby preserve long-term joint health. Abnormal cartilage loading patterns can disrupt tissue homeostasis and initiate degenerative pathways (Griffin and Guilak, 2005), which likely contributes to the high prevalence of early onset osteoarthritis (OA) among individuals with prior ACL and meniscal injuries (Andriacchi et al., 2004; Lohmander et al., 2007). Thus, restoration of normative soft tissue loading patterns is an important objective for long-term success of treatments for ACL and meniscal injuries.

A subset of ACL deficient patients, termed "copers", restore knee stability through altered neuromuscular coordination (Schenk et al., 2014). Because the ACL is a primary passive restraint to tibial anterior translation and internal rotation (Moewis et al., 2016), muscular restraint must mitigate the corresponding increase in knee laxity to compensate for ACL deficiency. Dynamic *in vivo* imaging studies report greater tibial anterior translation, medial translation and internal rotation during an array of tasks such as active knee flexion, lunging, and walking in ACL deficient patients (DeFrate et al., 2006; Isaac et al., 2005; Stergiou et al., 2007; Waite et al., 2005). However, substantial inter-subject variability is present, with select patients exhibiting relatively normal tibiofemoral kinematic patterns during active knee flexion-extension (Barrance et al., 2007). The underlying factors that enable neuromuscular compensation for ACL deficiency remain elusive, as electromyography (EMG) evidence suggests there is a variety of adaptations across the coper population (Alkjaer et al., 2003; Macleod, 2014; Rudolph et al., 2001; Schenk et al., 2014).

The meniscus distributes loading across the cartilage surface and provides secondary restraint to the tibiofemoral joint

☆ The first author (CRS) is the winner of the 2017 American Society of Biomechanics Young Scientist Pre-doctoral Award.

* Corresponding author at: Department of Mechanical Engineering, 1513 University Avenue, Madison, WI 53706, USA.
E-mail address: dgthelen@wisc.edu (D.G. Thelen).

https://doi.org/10.1016/j.jbiomech.2018.10.008
0021-9290/

(McDermott et al., 2008). Damage to the meniscus changes the articular contact geometry, resulting in altered contact pressure distributions that are not likely to be restored through altered neuromuscular coordination. However, active muscle forces might supplement the diminished joint restraint of a damaged meniscus. This is functionally important since meniscectomy can elevate ACL strain (Spang et al., 2010) and predispose both the native ACL and reconstructed ACL to injury (Papageorgiou et al., 2001; Trojani et al., 2011). Thus, a possible goal for conservative treatment of meniscal damage would focus neuromuscular training to develop a coordination strategy that prevents overloading the ACL. Currently, it is uncertain whether this goal is mechanically achievable.

Musculoskeletal simulation enables systematic investigation of the dynamic coupling between neuromuscular coordination and knee joint mechanics. However, prior simulation studies are conflicting as to whether neuromuscular coordination can restore normative knee mechanics in ACL deficient patients. Simulations of open-chain knee extension tasks suggest that hamstring co-contraction reduces ACL loading (O'Connor, 1993) and can restore anterior translation patterns in an ACL deficient knee (Yanagawa et al., 2002). Some simulations of walking suggest that elevated hamstring activation can restore anterior tibial translation to normative ranges (Liu and Maitland, 2000; Shelburne et al., 2005a). However, other predictions indicate that hamstrings co-activation cannot fully restore anterior tibial translation to normative patterns (Shao et al., 2011). These studies provide insights into the functional role of muscles in compensating for ACL deficiency, but are limited by modeling simplifications including two dimensional analyses, lack of a meniscus, and an inability to explicitly study cartilage loading patterns.

This study investigates the differences in soft tissue loading patterns caused by ACL and menisci deficiency and whether these differences can be mitigated through an altered neuromuscular coordination strategy. The first objective was to identify the differences in tibiofemoral kinematics and cartilage and ligament loading patterns during walking for intact, ACL deficient, menisci deficient, and ACL-menisci deficient knees. The second objective was to investigate the feasibility of modulating neuromuscular coordination to restore normative kinematics and cartilage loading patterns in ACL deficient knees and ACL loading in menisci deficient knees.

2. Methods

A multibody knee model of a healthy female subject (Age = 23, Height = 1.65 m, Mass = 61 kg) was previously constructed from magnetic resonance images (MRI) (Lenhart et al., 2015). The predictive capacity of the model was evaluated by comparing simulated knee kinematics against measured kinematics from dynamic MRI during active and passive knee flexion-extension. For this study, the model included femur, tibia, and patella bodies, and independent medial and lateral menisci bodies that floated on the tibial plateau. Each joint in the knee model allowed six degrees-of-freedom (DOF) of relative motion. Articular contact (cartilage-cartilage ($E = 5$ MPa, $\nu = 0.45$) and cartilage-meniscus ($E = 3$ MPa, $\nu = 0.45$)) was modeled using an elastic foundation formulation (Bei and Fregly, 2004; Smith et al., 2016). Ligament and capsular structures spanning the tibiofemoral and patellofemoral joints were represented by fourteen bundles of nonlinear springs (Blankevoort and Huiskes, 1991). The menisci were tethered to the tibia via nonlinear spring representations of the anterior and posterior meniscal horns, transverse ligament, and circumferential attachment of the menisci to the tibial plateau. The knee was integrated into a scaled generic lower extremity model that included 44 muscles (Arnold et al., 2010).

Skin mounted marker kinematics and ground reactions were measured for the subject during overground walking (1.2 m/s) in a motion analysis laboratory. The protocol for this experiment was approved by the University of Wisconsin Institutional Review Board. A global optimization inverse kinematics routine was used to calculate the trajectories of the six *prescribed* (6-pelvis) and five

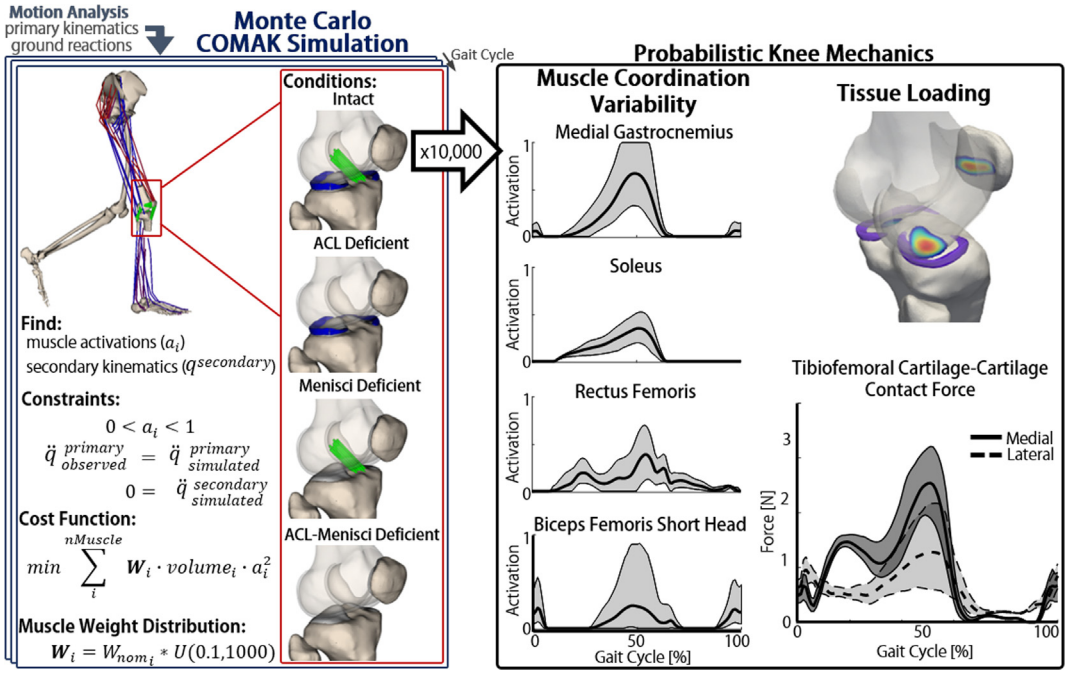

Fig. 1. The COMAK simulation framework was used to predict the *secondary* knee kinematics, muscle forces, ligament forces, and articular contact pressures necessary to generate the measured motion. Simulations were performed using the same input gait measurements for four knee conditions: intact, ACL deficient, menisci deficient and ACL-menisci deficient. For the intact, ACL deficient and menisci deficient conditions, a Monte Carlo analysis (10,000 simulations) was performed in which the weightings on each muscle in the COMAK cost function were varied to generate neuromuscular coordination patterns to explore the solution space of muscle redundancy.

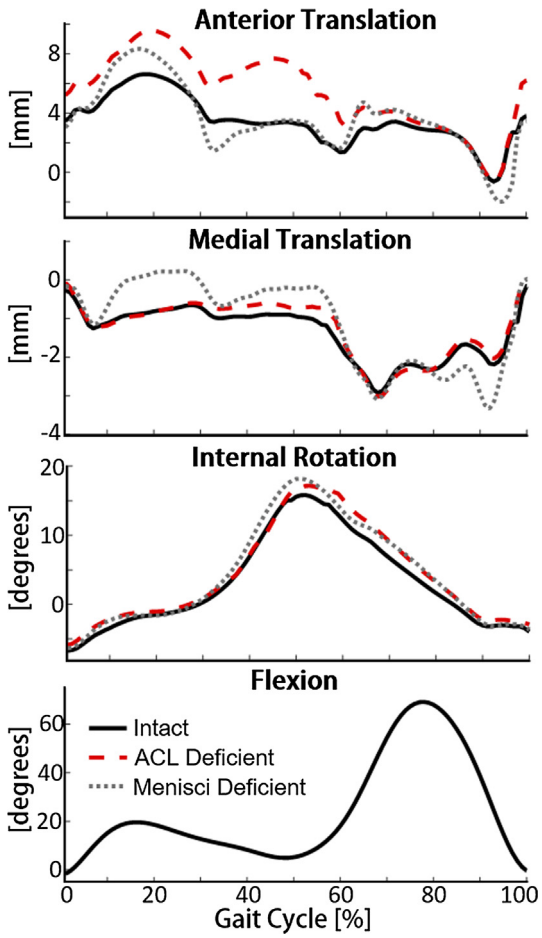

Fig. 2. For each knee condition, the flexion angle was set to the measured value, while the *secondary* knee kinematics (e.g. anterior tibial translation, medial tibial translation and internal tibial rotation) were predicted by the COMAK algorithm.

primary (3-hip, 1-tibiofemoral flexion, 1-ankle) lower extremity DOFs. During the inverse kinematics procedure, the 23 *secondary* knee DOFs (5-tibiofemoral, 6-patellofemoral and 12-meniscal) were constrained to be functions of tibiofemoral flexion. These functions were determined from a forward simulation in which the muscles were minimally activated (2%) and tibiofemoral flexion was prescribed from 0° to 120° while the *secondary* kinematics were unconstrained.

The Concurrent Optimization of Muscle Activations and Kinematics (COMAK) algorithm was then used to predict the muscle forces, *secondary* knee kinematics, ligament forces, and articular contact pressures necessary to reproduce the measured accelerations of the *primary* DOFs during walking (Brandon et al., 2017) (Fig. 1). At each time step, the *prescribed* and *primary* lower extremity DOF were set to the measured values. The muscle activations and *secondary* kinematics were then optimized to generate the measured accelerations for the *primary* DOFs and equilibrium (zero accelerations) in the *secondary* DOFs while minimizing a cost function (J). The cost function was the muscle volume (V_i) weighted sum of squared muscle activations (a_i) and included muscle specific weighting terms (W_i).

$$J = \sum_{i=1}^{nMuscles} W_i * V_i * a_i^2 \quad (1)$$

The muscle weights penalize the activation of a muscle if ($W_i > 1$) and encourage the activation if ($W_i < 1$) in the solution to muscle redundancy. The nominal muscle weight for each muscle was set equal to one ($W_i = 1$), except for the medial gastrocnemius ($W_i = 4$), lateral gastrocnemius ($W_i = 7$), hamstrings ($W_i = 2$), rectus femoris ($W_i = 3$), soleus ($W_i = 0.9$), gluteus minimus ($W_i = 0.9$), and gluteus medius ($W_i = 0.9$). These weightings were selected to reduce the knee contact force in the nominal simulation to physiologic magnitudes (DeMers et al., 2014; Steele et al., 2012).

Four gait simulations using intact, ACL deficient, menisci deficient, and ACL-menisci deficient conditions in the knee model were generated using the nominal weighting factors. In addition, we explored the muscle redundancy solution space using a Monte Carlo analysis where the muscle weights (W_i) were randomly varied for gait simulations generated for the intact, ACL deficient, and menisci deficient conditions. Muscle weights were parameterized as uniform distributions spanning from 10 to 10,000% of the nominal weight (W_i) value. The bounds on the distributions were determined as the largest range that still enabled all simulations to converge. A high throughput computing grid was used to perform 10,000 simulations for each condition. The mean values of the predicted kinematics and cartilage loading metrics were less than 1% different when calculated using 9,000 vs 10,000 simulations, ensuring an adequate number of simulations were performed (Ballio and Guadagnini, 2004). Two additional sets of 10,000 simulations were performed with the ACL deficient knee with a lower bound on the hamstrings activations set to 20% and 40% within the COMAK optimization. This constraint enabled investigation of the function of enhanced hamstring recruitment during stance.

For each condition, the predicted anterior tibial translation, internal tibial rotation, tibiofemoral cartilage contact pressure magnitudes and locations, and ACL loading were compared. The variability in joint mechanics induced by different neuromuscular coordination strategies was quantified by calculating the mean, and 5th and 95th percentiles of each metric. The sensitivity of each metric to the activation of each muscle was determined by calculating the Spearman correlation coefficient (R) at the instances of the 1st and 2nd peaks in the tibiofemoral loading during stance.

3. Results

Simulated tibiofemoral contact forces during gait demonstrated the characteristic double peak (1st peak: 17%, 2nd peak: 48% gait cycle) (Fig. 1). Anterior tibial translation and ACL loading were greatest at 1st peak, which also coincides with peak quadriceps activation. The predicted internal rotation increased throughout stance, with peak internal rotation (15.8°) occurring slightly before toe-off.

3.1. Nominal gait simulation with ACL deficient knee

Simulated ACL deficiency substantially altered *secondary* knee kinematics during gait relative to the nominal predictions for the intact knee. The tibia shifted anteriorly in terminal swing. This anterior shift persisted throughout stance and early swing, before converging back to the normative pattern at mid-swing (Fig. 2). The maximum increase in anterior translation (3 mm) occurred in early stance when the quadriceps activation was greatest. The ACL deficient knee also exhibited increased internal rotation at push off, which persisted throughout the swing phase, and increased medial translation during the second half of stance.

Simulated cartilage loading patterns for the ACL deficient knee were also substantially altered relative to the intact condition (Fig. 3, Supplemental Fig. 1). At the 1st and 2nd peaks of tibiofemoral loading, the anterior location of the center of pressure (COP) on the medial tibial plateau was 1.7 mm and 2.3 mm posterior to the intact COP, respectively. On the lateral tibial plateau, the COP was 1.8 mm and 0.4 mm posterior. The mean cartilage-

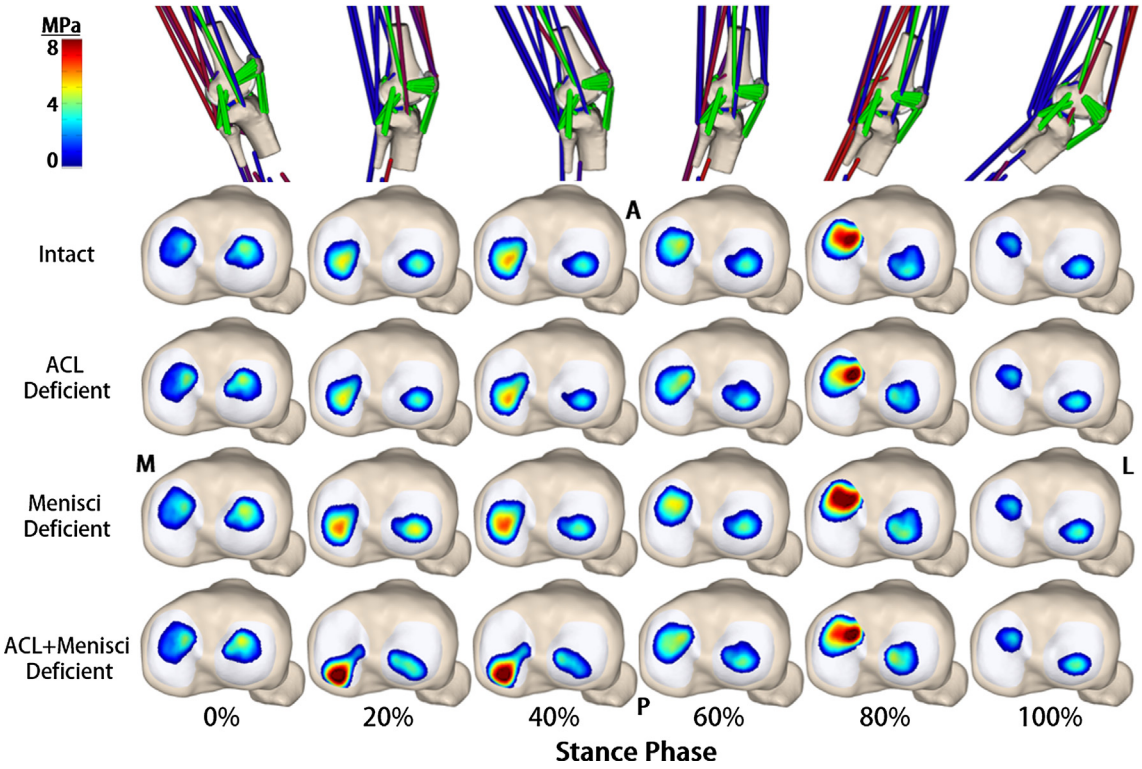

Fig. 3. A comparison of tibial cartilage-cartilage contact pressure patterns for each condition over the stance phase of walking. Pressure maps at the 1st peak of tibiofemoral loading (17% gait cycle, 28% stance) are shown in Fig. 8. The 2nd peak of tibiofemoral loading (48% gait cycle, 72% stance) demonstrates similar pressure patterns to the 80% column. The muscle activations (red-active, blue-inactive) and knee kinematics for the nominal simulation of the intact condition are visualized at the top of the figure. Femoral cartilage-cartilage contact pressure patterns are shown in Supplemental Fig. 1. (For interpretation of the references to color in this figure legend, the reader is referred to the web version of this article.)

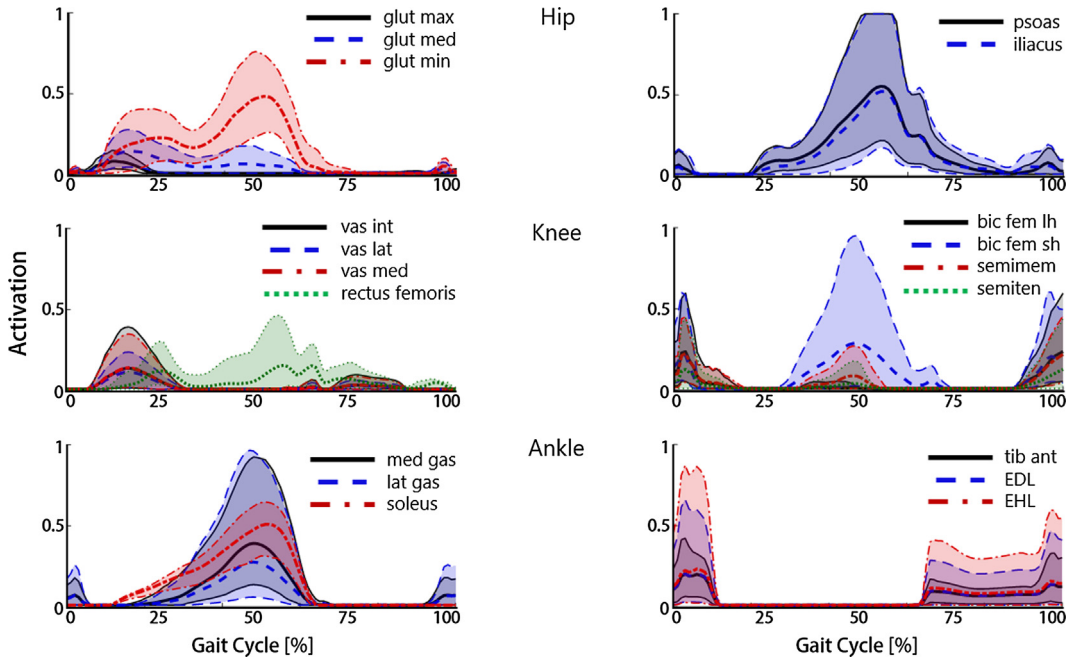

Fig. 4. A summary of the exploration of muscle redundancy solution space where the mean (bold center line) and 5–95 percentiles (shaded region) of the muscle activation patterns predicted in the 10,000 simulations with variable muscle weight factors for the ACL deficient condition. The intact and menisci deficient conditions resulted in similar temporal patterns with slightly different magnitudes for select muscles. Additional simulations were performed with minimal prescribed minimal hamstrings activations to ensure full exploration of the muscle redundancy solution space (Fig. 9). EDL: extensor digitorum longus, EHL: extensor hallucis longus.

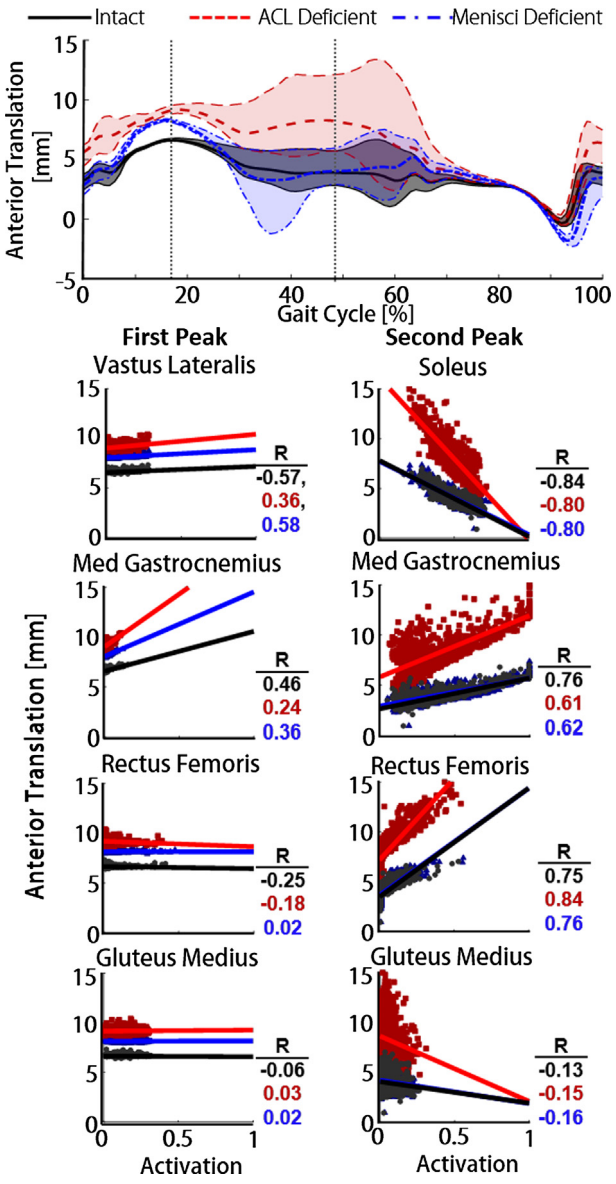

Fig. 5. [Top Plot] The results of each batch of 10,000 simulations is summarized by the mean (bold centerline) and 5th-95th percentiles (shaded region) of anterior tibial translation over the gait cycle for each condition. The dotted vertical lines depict the instances of the 1st and 2nd peaks of tibiofemoral loading. [Scatter Plots] The scatter plots reveal the sensitivity of anterior translation to activation of each muscle at the 1st and 2nd peaks in tibiofemoral loading. The best fit line and Spearman correlation coefficient were calculated for the intact (black), ACL deficient (red) and menisci deficient (blue) conditions. (For interpretation of the references to color in this figure legend, the reader is referred to the web version of this article.)

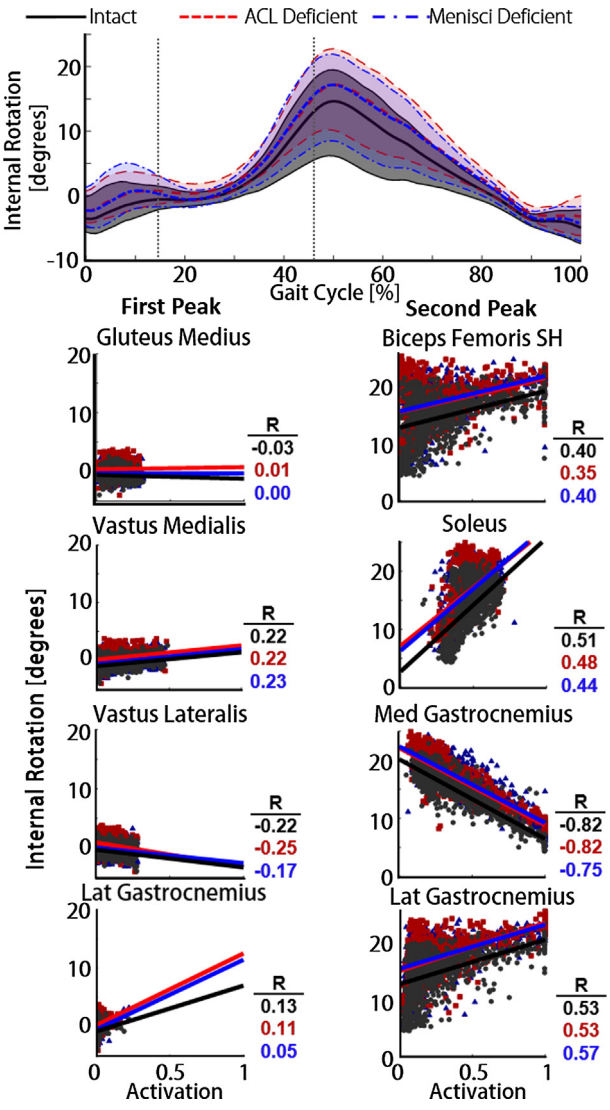

Fig. 6. [Top Plot] The mean (bold center line) and 5th-95th percentiles of the internal rotation for the variable neuromuscular coordination simulations are plotted over the gait cycle. The dotted vertical lines coincide with the 1st and 2nd peaks of tibiofemoral loading. [Scatter plots] The sensitivity of predicted internal rotation at the 1st and 2nd peaks to the activation of each muscle was quantified using Spearman's correlation coefficient for the intact (black), ACL deficient (red), and menisci deficient (blue) conditions. (For interpretation of the references to color in this figure legend, the reader is referred to the web version of this article.)

cartilage contact pressure was slightly lower on both plateaus at 1st peak in the ACL deficient knee compared to the intact knee condition resulting from a greater proportion of the contact force shifting onto the meniscus (Supplemental Fig. 2).

Supplementary data associated with this article can be found, in the online version, at https://doi.org/10.1016/j.jbiomech.2018.10.008.

3.2. Nominal gait simulation with menisci deficient knee

The menisci deficient knee experienced considerably higher cartilage-cartilage contact pressures and increased loading in the remaining passive knee structures. At 1st peak, the mean cartilage contact pressures on the tibial plateau were increased by 18% and 24%, respectively, compared to the intact condition. Menisci deficiency resulted in an anterior shift of the tibia in early stance, and a posterior shift in late stance (Fig. 2). There was also an increase in the internal rotation and medial translation during stance. The medial tibial COP was shifted 1.5 mm posteriorly at 1st peak and 0.6 mm anteriorly at 2nd peak compared to the intact condition. The lateral tibial COP was 0.5 mm anterior at 1st peak and 0.6 mm anterior at the 2nd peak. The loading in the ACL was 2.4× higher in the meniscus deficient knee compared to the intact knee at the instance of peak quadriceps loading.

3.3. Nominal gait simulation with ACL-menisci deficient

The ACL-menisci deficient knee lacked passive restraint to anterior loads, resulting in substantially greater anterior translation at 1st peak when the quadriceps were active. At this instance, the contact shifted to the posterior edge of the tibial plateau resulting in greatly elevated contact pressures (Fig. 3).

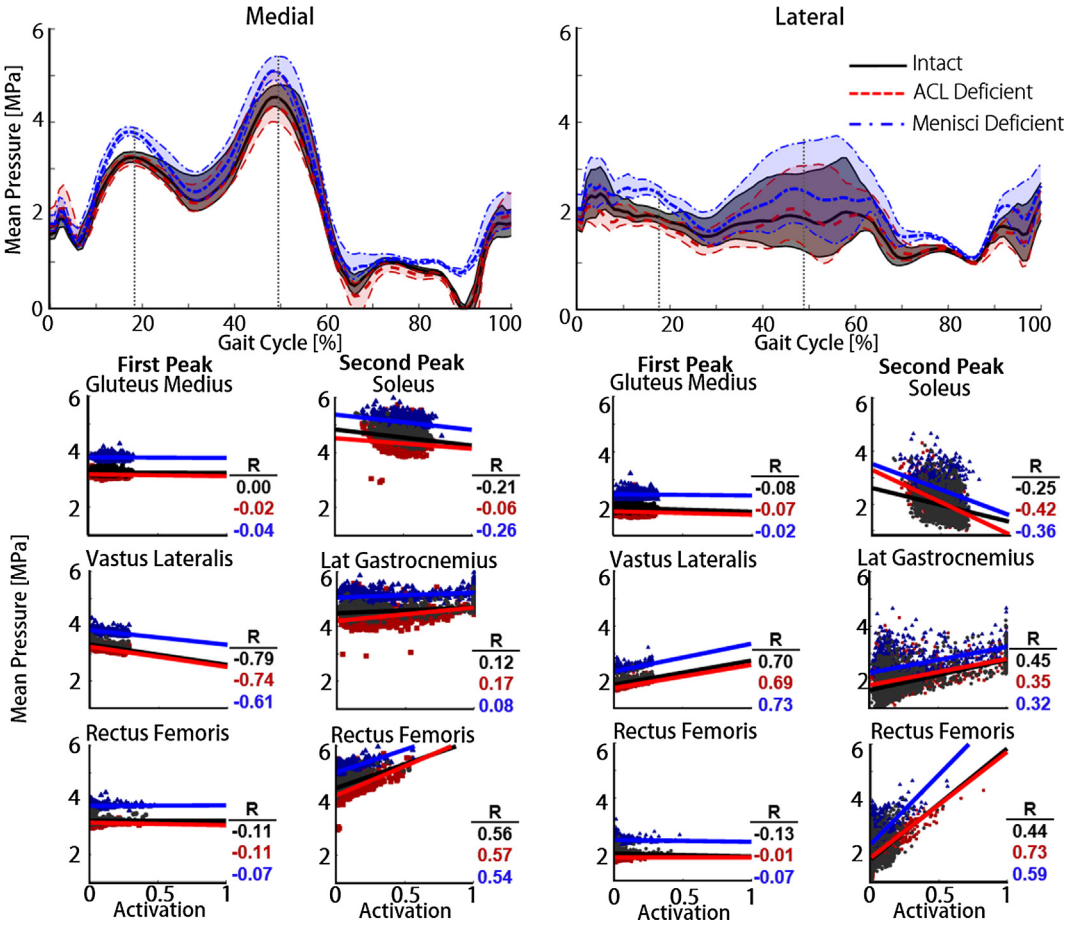

Fig. 7. [*Top Plot*] The mean (bold centerline) and 5th-95th percentiles (shaded) of the cartilage-cartilage contact pressures on the medial and lateral tibial plateaus are shown for variable neuromuscular coordination simulations for each condition. The vertical dotted lines indicate the 1st and 2nd peaks of tibiofemoral loading. [*Scatter plots*] The sensitivity of the mean cartilage-cartilage contact pressures was accessed at the 1st and 2nd peaks of tibiofemoral loading using the Spearman correlation coefficient (R).

3.4. Influence of neuromuscular coordination

The muscle weightings within the COMAK cost function influenced the predicted muscle activations (Fig. 4), knee kinematics (Figs. 5 & 6), cartilage contact pressures (Fig. 7), and ACL forces (Fig. 8) during walking. Variability in predicted knee mechanics from heel strike through 1st peak was substantially less than the variability present from 2nd peak through toe off and early swing. However, cartilage loading in the ACL deficient knee was not restored to normative patterns by any of the 10,000 muscle coordination strategies. The absent mechanical restraint of the ACL resulted in increased anterior tibial translation for all coordination patterns, particularly during stance (Fig. 5). In late stance, preferential activation of the soleus compared to the gastrocnemii reduced the anterior translation, but did not fully restore normative anterior translation patterns. However, the internal rotation could be restored to normative patterns by preferentially activating the lateral vastus compared to medial vastus during load acceptance, and the medial gastrocnemius over the lateral gastrocnemius during push-off (Fig. 6). The mean cartilage-cartilage contact pressures were generally similar to the intact knee (Fig. 7). Surprisingly, the cases of imposed minimum 20% and 40% hamstrings activation resulted in increases of anterior tibial translation of 1.5 mm and 4.3 mm at 1st peak compared to the unconstrained case in the ACL deficient knee (Fig. 9).

In the menisci deficient knee, the mean cartilage-cartilage contact pressures were generally higher than the intact and ACL deficient knees regardless of the muscle coordination pattern (Fig. 7). This was especially true at the first peak of tibiofemoral loading where there was no overlap between the medial and lateral pressure ranges for the intact and menisci deficient conditions. The altered neuromuscular coordination strategies could not restore ACL loading to intact magnitudes in the menisci deficient knee during the first half of stance phase when the quadriceps were active (Fig. 8).

4. Discussion

We used musculoskeletal simulation to investigate the differences in cartilage loading patterns during walking between intact, ACL deficient, menisci deficient, and ACL-menisci deficient knees. Then, we tested whether altered neuromuscular coordination strategies could restore normative soft tissue loading patterns in the pathologic knees. In the ACL deficient knee, we predicted increased anterior tibial translation, resulting in a posterior shift in the medial tibial cartilage contact and increased load on the menisci during load acceptance. In the menisci deficient knee, we found a minor posterior shift in the medial contact and a substantial increase in cartilage contact pressure. In the ACL-menisci deficient knee, the cartilage contact shifted to the extreme posterior boundary of the tibial cartilage, resulting in heightened contact pressures. Altered neuromuscular coordination was unable to restore the cartilage contact locations during stance in the ACL deficient knee. Neither cartilage contact pressure magnitudes nor

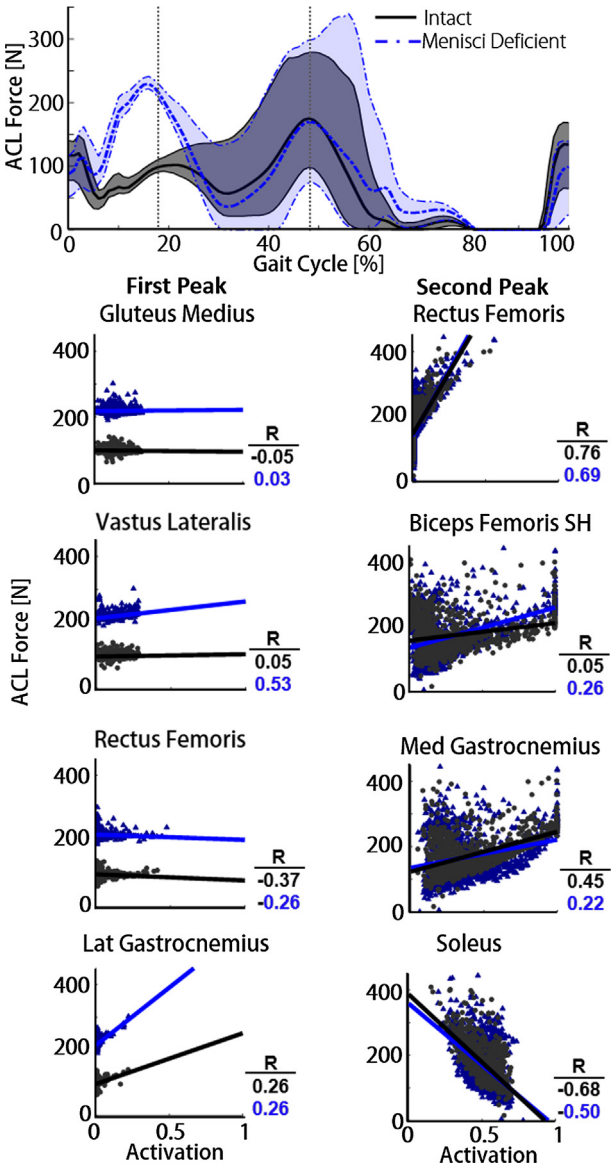

Fig. 8. [*Top Plot*] The mean (bold centerline) and 5th to 95th percentiles (shaded) of ACL force for the variable neuromuscular coordination simulations of the intact (black) and menisci deficient (blue) knees. The vertical dotted lines indicate the instances of 1st and 2nd peaks of tibiofemoral loading. [*Scatter Plots*] The sensitivity of ACL force to muscle activations at 1st and 2nd peaks is assessed through the Spearman correlation coefficient (R). (For interpretation of the references to color in this figure legend, the reader is referred to the web version of this article.)

ACL loading were restored by modulating coordination in the menisci deficient condition.

The regions of altered cartilage contact pressure patterns in the injured conditions at the 1st peak of tibiofemoral loading (also peak ACL loading in the intact knee, 18% of gait cycle) corresponded well with reported regions of cartilage wear (Fig. 10). Three studies examining tibial plateau resections from total knee replacements found a posterior shift and increased area of wear patterns on the medial plateau in ACL deficient knees compared to ACL intact knees (Harmon and Markovich, 1998; Moschella et al., 2006; Mullaji et al., 2008). We found a posterior shift in the medial tibial COP in the ACL deficient knee compared to intact at the instance of peak ACL loading (1st peak). Moschella reported that severe cartilage wear was found on the posterior lateral corner of the medial plateau in 20% of ACL deficient knees and 46% of ACL-menisci deficient knees (Moschella et al., 2006). We found the contact pressures increased substantially in this region with the removal of the menisci in the ACL deficient knee. These comparisons support the notion that shifts in cartilage loading patterns due to soft tissue injury are an important contributor to cartilage wear patterns seen in osteoarthritic knees.

Altered neuromuscular coordination had substantial effects on tissue loading during the second half of stance. This variability was caused by a redistribution of the hip, knee, and ankle joint moments between uniarticular and biarticular muscles (DeMers et al., 2014). The distribution of the hip flexion moment between the uniarticular muscles and the rectus femoris, and the distribution of the ankle plantarflexion moment between the soleus and gastrocnemii had significant ramifications at the knee. Coordination strategies that favored the rectus femoris to generate the hip flexion moment and gastrocnemii to generate the knee flexion and ankle plantar flexion moments resulted in the largest anterior tibial translations, cartilage contact pressures, and ACL loads. For example, if the ankle plantarflexion moment was generated by the gastrocnemii rather than the soleus, increased contact force and anterior translation occurred at the knee. If the hip flexion moment was generated by the rectus femoris, an extension moment was applied to the knee which had to be overcome by the gastrocnemii and hamstrings, resulting in increased contact force and anterior translation.

There was minimal overlap between the predicted anterior tibial translation ranges due to varied neuromuscular coordination in the intact and ACL deficient knees (Fig. 5). As a result, locations of cartilage loading at 1st peak could not be restored through altered neuromuscular coordination in the ACL deficient knee. Regardless of coordination strategy, the cartilage contact pressures (Fig. 7) and ACL loads (Fig. 8) in the menisci deficient knee were always elevated during load acceptance relative to the intact condition. The larger contact pressures were a result of the reduced contact area (Kim and Park, 1993). ACL loads were elevated because of the loss of the secondary contribution of the menisci as a restraint to anterior translation. These results suggest that adaptations in neuromuscular coordination alone are insufficient to mitigate abnormal soft tissue loading due to injury to the ACL or menisci.

The simulations with imposed minimal hamstrings activity revealed that co-contraction of the hamstrings counterintuitively leads to increased anterior translation of the tibia in the ACL deficient knee. This result contradicts *in vivo* (Fleming et al., 2001) and cadaver experiments (More et al., 1993) under simple loading conditions. Yet, it can be explained by two factors: (1) the quadriceps activations must be elevated to overcome the co-activated hamstrings flexion moment, (2) the resulting increased anterior load of the patellar tendon exceeds the imposed anterior restraint of the hamstrings at moderate knee flexion angles (Aalbersberg et al., 2005; Herzog and Read, 1993; Hirokawa et al., 1991). Thus, the commonly reported ACL agonist role of the hamstrings may not extend to walking where external loading dictates a net internal knee extension moment during load acceptance while the knee is in an extended posture.

The interaction of muscle lines of action and limb dynamics highlighted by our simulations suggests two movement compensations that may contribute to restoring anterior tibial translation in the ACL deficient knee. First, using a more flexed knee posture would provide more advantageous muscle lines of action to reduce anterior translation. Cadaver studies indicate the anterior component of the patellar tendon force is greatest at full extension and reduces with flexion (Herzog and Read, 1993; Victor et al., 2010). The hamstrings line of action is nearly vertical at full extension and becomes more posterior with increased flexion (Aalbersberg et al., 2005; Herzog and Read, 1993). This compensation appears to be present in some ACL deficient patients who exhibit increased knee flexion during walking compared to healthy controls (Alkjaer

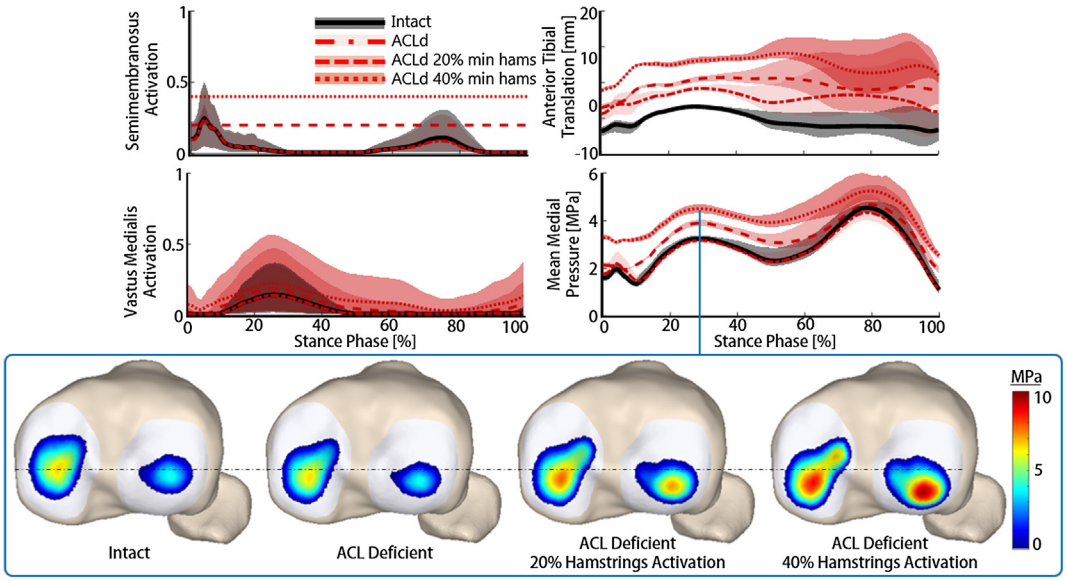

Fig. 9. A comparison of the intact, ACL deficient, and ACL deficient with minimum hamstrings activations of 20% and 40% conditions during the stance phase. Surprisingly, the imposed hamstrings activations increased the anterior tibial translation. This arises from the corresponding increases in quadriceps activation necessary to generate the extension moment dictated by the locomotion dynamics. The musculotendon geometry at moderate flexion angles results in the anterior component of the increased patellar tendon load overcoming the posterior component of the increased hamstrings load.

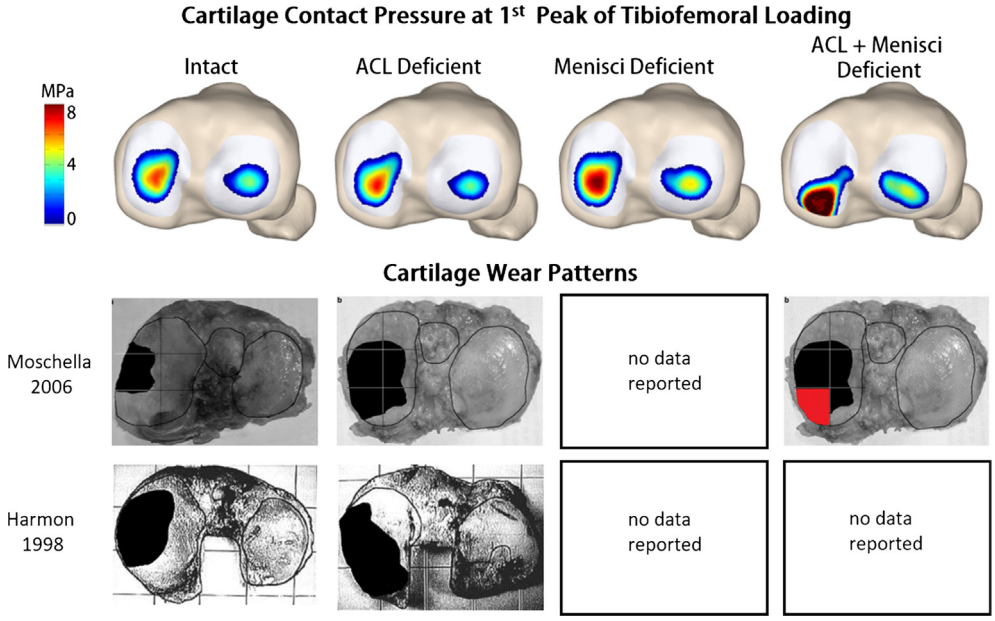

Fig. 10. Predicted cartilage contact pressures at the instance of 1st peak tibiofemoral loading (18% gait cycle) compared against wear patterns found on tibial resections from total knee replacement surgeries (Harmon and Markovich, 1998; Moschella et al., 2006). The black regions indicate representative wear patterns for each knee condition. The red coloring indicates a region where 20% of ACL deficient knees and 46% of ACL-menisci deficient knees showed severe cartilage wear. The cartilage wear pattern images have been reproduced with permission from Elsevier and Wolters Kluwer Health. (For interpretation of the references to colour in this figure legend, the reader is referred to the web version of this article.)

et al., 2003; Gao and Zheng, 2010; Patel et al., 2003; Schenk et al., 2014; Shabani et al., 2015), but not others who exhibit no difference or even reduced flexion (Georgoulis et al., 2003; Ismail et al., 2016; Rudolph et al., 2001; Wexler et al., 1998). The second potential compensation is a reduction of the internal knee extension moment in early stance. This adaptation has been widely reported in ACL deficient populations and thus may indicate ACL deficient patients modulate their movement dynamics to compensate for the injury (Berchuck et al., 1990; Noyes et al., 1992; Patel et al., 2003; Torry et al., 2004). Our simulations presumed the same input gait kinematics and kinetics for both intact and ACL deficient knees, which may be representative of the coper population who exhibit similar movement patterns to healthy controls (Rudolph et al., 2001). Further study is needed to ascertain how variations in movement patterns may modulate the influence of neuromuscular coordination on internal mechanics of ACL deficient knees.

Electromyography studies commonly report co-contraction in ACL deficient patients to "stabilize" the knee (Shanbehzadeh et al., 2017). Our simulations demonstrate that quadriceps, gastrocnemii, and hamstrings recruitment increase ACL loading if the movement dynamics are unaltered. Thus, co-contraction of the knee flexors and extensors to stabilize the knee will substantially increase

anterior translation and elevate the cartilage contact pressures. Over the range of simulated neuromuscular coordination strategies, the variable co-contraction led to ranges in mean medial pressure of 0.44 MPa at 1st peak, and 1.69 MPa at 2nd peak. When minimal hamstrings activations of 20% and 40% were imposed, the mean medial cartilage-cartilage contact pressure increased by 18% and 36%, respectively (Fig. 9). This reinforces the hypothesis that co-contraction may stiffen the joint, but also leads to higher contact loads which may be detrimental to the long-term health of the cartilage tissue (Rudolph et al., 1998; Sharifi et al., 2017).

Our predictions of increased anterior tibial translation in the ACL deficient knee during stance and convergence to the intact pattern during mid-swing are in agreement with previous simulation (Shao et al., 2011; Shelburne et al., 2004) and experimental studies (Andriacchi and Dyrby, 2005). However, we kept the overall movement dynamics constant across all simulations, which revealed the counterintuitive ACL antagonist role of the hamstrings during walking, which conflicts with previous simulation results (Liu and Maitland, 2000; Pandy and Shelburne, 1997; Shao et al., 2011; Shelburne et al., 2005b). In agreement with previous studies, we also showed that the gastrocnemii are ACL antagonists (Adouni et al., 2016; Fleming et al., 2001). The soleus has previously been proposed as an agonist to the ACL due to its posterior force application to the tibia (Colné and Thoumie, 2006; Elias et al., 2003; Hurd and Snyder-Mackler, 2007; Mokhtarzadeh et al., 2013). Our simulations confirm the soleus to be an ACL agonist, but this function was mainly due to the corresponding reduction in the gastrocnemii force necessary to generate the ankle plantarflexion moment during push-off.

Our application of the COMAK simulation framework to study muscle coordination in ACL and menisci injury has several limitations. We used experimental gait data and a knee model from a single healthy subject. However, both knee geometry (Shao et al., 2011) and limb dynamics (Shelburne et al., 2003) are known to influence the joint mechanics in ACL deficient knees. Additionally, we performed our analyses using a single set of ligament stiffnesses and slack lengths. We recognize that there is uncertainty in these parameters (Laz et al., 2007) and that they vary among the population (Chandrashekar et al., 2006) in a manner that will affect predictions of internal knee mechanics (Smith et al., 2015). However, despite the potential impact of these limitations on the magnitude and precision of quantitative conclusions, our probabilistic modeling framework revealed general relationships between joint injury, muscle function, and joint mechanics that are consistent with experimental data.

In conclusion, we found that simulated tibiofemoral cartilage contact pressures were elevated in regions where cartilage wear patterns are observed in both ACL deficient and menisci deficient knees. Varying neuromuscular coordination was insufficient to fully restore normative cartilage loading in either ACL deficient or menisci deficient conditions, but did substantially modulate contact pressure magnitudes and patterns during the late stance phase of walking. These insights are important for evaluating treatment and rehabilitation strategies for knee ligament and meniscus damage.

Conflict of interest

The authors declare that there are no conflict of interest.

Acknowledgements

Funding for this research was provided by NIH grant EB015410.

References

Aalbersberg, S., Kingma, I., Ronsky, J.L., Frayne, R., Van Dieën, J.H., 2005. Orientation of tendons in vivo with active and passive knee muscles. J. Biomech. 38, 1780–1788. https://doi.org/10.1016/j.jbiomech.2004.09.003.

Adouni, M., Shirazi-Adl, A., Marouane, H., 2016. Role of gastrocnemius activation in knee joint biomechanics: gastrocnemius acts as an ACL antagonist. Comput. Methods Biomech. Biomed. Eng. 19, 376–385. https://doi.org/10.1080/10255842.2015.1032943.

Alkjaer, T., Simonsen, Æ.E.B., Jørgensen, Æ.U., Dyhre-poulsen, P., 2003. Evaluation of the walking pattern in two types of patients with anterior cruciate ligament deficiency: copers and non-copers. Eur. J. Appl. Physiol. 89, 301–308. https://doi.org/10.1007/s00421-002-0787-x.

Andriacchi, T.P., Dyrby, C.O., 2005. Interactions between kinematics and loading during walking for the normal and ACL deficient knee. J. Biomech. 38, 293–298. https://doi.org/10.1016/j.jbiomech.2004.02.010.

Andriacchi, T.P., Mündermann, A., Smith, R.L., Alexander, E.J., Dyrby, C.O., Koo, S., 2004. A framework for the in vivo pathomechanics of osteoarthritis at the knee. Ann. Biomed. Eng. 32, 447–457.

Arnold, E.M., Ward, S.R., Lieber, R.L., Delp, S.L., 2010. A model of the lower limb for analysis of human movement. Ann. Biomed. Eng. 38, 269–279. https://doi.org/10.1007/s10439-009-9852-5.A.

Ballio, F., Guadagnini, A., 2004. Convergence assessment of numerical Monte Carlo simulations in groundwater hydrology. Water Resour. Res. 40, 1–5. https://doi.org/10.1029/2003WR002876.

Barrance, P., Williams, G., Snyder-Mackler, L., Buchanan, T., 2007. Do ACL-injured copers exhibit differences in knee kinematics?: an MRI study. Clin. Orthop. Relat. Res. 454, 74–80. https://doi.org/10.1097/BLO.0b013e31802bab0d.

Bei, Y., Fregly, B.J., 2004. Multibody dynamic simulation of knee contact mechanics. Med. Eng. Phys. 26, 777–789. https://doi.org/10.1016/j.medengphy.2004.07.004.

Berchuck, M., Andriacchi, T.P., Bach, B.R., Reider, B., 1990. Gait adaptations by patients who have a deficient anterior cruciate ligament. J. Bone Jt. Surg., 871–877

Blankevoort, L., Huiskes, R., 1991. Ligament-bone interaction in a three-dimensional model of the knee. J. Biomech. Eng. 113, 263–269.

Brandon, S.C.E., Smith, C.R., Thelen, D.G., 2017. Simulation of Soft Tissue Loading from Observed Movement Dynamics. In: Handbook of Human Motion. pp. 1–34. <https://doi.org/10.1007/978-3-319-30808-1_172-1>

Chandrashekar, N., Mansouri, H., Slauterbeck, J., Hashemi, J., 2006. Sex-based differences in the tensile properties of the human anterior cruciate ligament. J. Biomech. 39, 2943–2950. https://doi.org/10.1016/j.jbiomech.2005.10.031.

Colné, P., Thoumie, P., 2006. Muscular compensation and lesion of the anterior cruciate ligament: contribution of the soleus muscle during recovery from a forward fall. Clin. Biomech. 21, 849–859. https://doi.org/10.1016/j.clinbiomech.2006.04.002.

DeFrate, L.E., Papannagari, R., Gill, T.J., Moses, J.M., Pathare, N.P., Li, G., 2006. The 6 degrees of freedom kinematics of the knee after anterior cruciate ligament deficiency. Am. J. Sports Med. 34, 1240–1246. https://doi.org/10.1177/0363546506287299.

DeMers, M.S., Pal, S., Delp, S.L., 2014. Changes in tibiofemoral forces due to variations in muscle activity during walking. J. Orthop. Res. 32, 769–776. https://doi.org/10.1002/jor.22601.

Elias, J.J., Faust, A.F., Chu, Y.-H., Chao, E.Y., Cosgarea, A.J., 2003. The soleus muscle acts as an agonist for the anterior cruciate ligament: an in vitro experimental study. Am. J. Sport. Med. 31, 241–246. https://doi.org/10.1177/03635465030310021401.

Fleming, B.C., Renstrom, P.a., Ohlen, G., Johnson, R.J., Peura, G.D., Beynnon, B.D., Badger, G.J., 2001. The gastrocnemius muscle is an antagonist of the anterior cruciate ligament. J. Orthop. Res. 19, 1178–1184. https://doi.org/10.1016/S0736-0266(01)00057-2.

Gao, B., Zheng, N.(Nigel), 2010. Alterations in three-dimensional joint kinematics of anterior cruciate ligament-deficient and -reconstructed knees during walking. Clin. Biomech. 25, 222–229. https://doi.org/10.1016/j.clinbiomech.2009.11.006.

Georgoulis, A.D., Papadonikolakis, A., Papageorgiou, C.D., Mitsou, A., Stergiou, N., 2003. Three-dimensional tibiofemoral kinematics of the anterior cruciate ligament-deficient and reconstructed knee during walking. Am. J. Sports Med. 31, 75–79. https://doi.org/10.1177/03635465030310012401.

Griffin, T.M., Guilak, F., 2005. The role of mechanical loading in the onset and progression of osteoarthritis. Exerc. Sport Sci. Rev. 33, 195–200.

Harmon, M., Markovich, G., 1998. Wear patterns on tibial plateaus from varus and valgus osteoarthritic knees. Clin. Orthop. Relat. Res. 352, 149–158.

Herzog, W., Read, L.J., 1993. Lines of action and moment arms of the major force-carrying structures crossing the human knee joint. J. Anat. 182 (Pt 2), 213–230.

Hirokawa, S., Solomonow, M., Luo, Z., Lu, Y., Ambrosia, R.D., 1991. Muscular co-contraction and control of knee stability. J. Electromyogr. Kinesiol. 1, 199–208.

Hurd, W.J., Snyder-Mackler, L., 2007. Knee instability after acute ACL rupture affects movement patterns during the mid-stance phase of gait. J. Orthop. Res. 25, 1369–1377. https://doi.org/10.1002/jor.20440.

Isaac, D.L., Beard, D.J., Price, A.J., Rees, J., Murray, D.W., Dodd, C.A.F., 2005. In-vivo sagittal plane knee kinematics: ACL intact, deficient and reconstructed knees. Knee 12, 25–31. https://doi.org/10.1016/j.knee.2004.01.002.

Ismail, S.A., Button, K., Simic, M., Van Deursen, R., Pappas, E., 2016. Three-dimensional kinematic and kinetic gait deviations in individuals with chronic anterior cruciate ligament deficient knee: a systematic review and meta-

analysis. Clin. Biomech. 35, 68–80. https://doi.org/10.1016/j.clinbiomech.2016.04.002.
Kim, S.J., Park, I.H., 1993. In vitro study of contact area and pressure distribution in the human knee after partial and total meniscectomy. Int. Orthop. 17, 214–218.
Laz, P.J., Stowe, J.Q., Baldwin, M.A., Petrella, A.J., Rullkoetter, P.J., 2007. Incorporating uncertainty in mechanical properties for finite element-based evaluation of bone mechanics. J. Biomech. 40, 2831–2836. https://doi.org/10.1016/j.jbiomech.2007.03.013.
Lenhart, R.L., Kaiser, J., Smith, C.R., Thelen, D.G., 2015. Prediction and validation of load-dependent behavior of the tibiofemoral and patellofemoral joints during movement. Ann. Biomed. Eng. https://doi.org/10.1007/s10439-015-1326-3.
Liu, W., Maitland, M.E., 2000. The effect of hamstring muscle compensation for anterior laxity in the ACL-deficient knee during gait. J. Biomech. 33, 871–879. https://doi.org/10.1016/S0021-9290(00)00047-6.
Lohmander, L.S., Englund, P.M., Dahl, L.L., Roos, E.M., 2007. The long-term consequence of anterior cruciate ligament and meniscus injuries: osteoarthritis. Am. J. Sports Med. 35, 1756–1769. https://doi.org/10.1177/0363546507307396.
Macleod, T.D., 2014. Differences in neuromuscular control and quadriceps morphology between potential copers and noncopers following anterior cruciate ligament. Injury 44, 76–84. https://doi.org/10.2519/jospt.2014.4876.
McDermott, I.D., Masouros, S.D., Amis, A.A., 2008. Biomechanics of the menisci of the knee. Curr. Orthop. 22, 193–201. https://doi.org/10.1016/j.cuor.2008.04.005.
Moewis, P., Duda, G.N., Jung, T., Heller, M.O., Boeth, H., Kaptein, B., Taylor, W.R., 2016. The restoration of passive rotational tibio-femoral laxity after anterior cruciate ligament reconstruction. PLoS One 11, 1–14. https://doi.org/10.1371/journal.pone.0159600.
Mokhtarzadeh, H., Yeow, C.H., Hong Goh, J.C., Oetomo, D., Malekipour, F., Lee, P.V.S., 2013. Contributions of the Soleus and Gastrocnemius muscles to the anterior cruciate ligament loading during single-leg landing. J. Biomech. 46, 1913–1920. https://doi.org/10.1016/j.jbiomech.2013.04.010.
More, R.C., Karras, B.T., Neiman, R., Woo, S.L., Daniel, D.M., Diego, S., 1993. Hamstrings-an anterior cruciate ligament protagonist. Am. J. Sports Med. 21, 231–237. https://doi.org/10.1177/036354659302100212.
Moschella Blasi, D.A., Leardini, A., Ensini, A., Catani, F., 2006. Wear patterns on tibial plateau from varus osteoarthritic knees. Clin. Biomech. (Bristol, Avon) 21, 152–158. https://doi.org/10.1016/j.clinbiomech.2005.09.001.
Mullaji, A.B., Marawar, S.V., Luthra, M., 2008. Tibial articular cartilage wear in varus osteoarthritic knees: correlation with anterior cruciate ligament integrity and severity of deformity. J. Arthroplasty 23, 128–135. https://doi.org/10.1016/j.arth.2007.01.015.
Noyes, F.R., Saddemi, S.R., Weise, M., Schipplein, O.D., Andriacchi, T.P., 1992. The anterior cruciate ligament-deficient knee with varus alignment: an analysis of gait adaptations and dynamic joint loadings. Am. J. Sports Med. 20, 707–716. https://doi.org/10.1177/036354659202000612.
O'Connor, J.J., 1993. Can muscle co-contraction protect knee ligaments after injury or repair? J. Bone Jt. Surg. Br. 75, 41–48.
Pandy, M., Shelburne, K., 1997. Dependence of cruciate-ligament loading on muscle forces and external load. J. Biomech. 30, 1015–1024.
Papageorgiou, C.D., Gil, J.E., Kanamori, A., Fenwick, J.A., Woo, S.L., Fu, F.H., 2001. The biomechanical interdependence between the anterior cruciate ligament replacement graft and the medial meniscus. Am. J. Sports Med. 29, 226–231.
Patel, R.R., Hurwitz, D.E., Bush-Joseph, C.A., Bach, B.R., Andriacchi, T.P., 2003. Comparison of clinical and dynamic knee function in patients with anterior cruciate ligament deficiency. Am. J. Sports Med. 31, 68–74. https://doi.org/10.1177/03635465030310012301.
Rudolph, K.S., Axe, M.J., Buchanan, T.S., Scholz, J.P., Snyder-Mackler, L., 2001. Dynamic stability in the anterior cruciate ligament deficient knee. Knee Surg. Sport. Traumatol. Arthrosc. 9, 62–71. https://doi.org/10.1007/s001670000166.
Rudolph, K.S., Eastlack, M.E., Axe, M.J., Snyder-Mackler, L., 1998. 1998 Basmajian Student Award Paper Movement patterns after anterior cruciate ligament injury: a comparison of patients who compensate well for the injury and those who require operative stabilization. J. Electromyogr. Kinesiol. 8, 349–362. https://doi.org/10.1016/S1050-6411(97)00042-4.
Schenk, W., Schenk, W., Diercks, R.L., 2014. Atypical hamstrings electromyographic activity as a compensatory mechanism in anterior cruciate ligament deficie .... a typical hamstrings electromyographic activity as a compensatory mechanism in anterior cruciate ligament deficiency. <https://doi.org/10.1007/s001670100196>
Shabani, B., Bytyqi, D., Lustig, S., Cheze, L., Bytyqi, C., Neyret, P., 2015. Gait changes of the ACL-deficient knee 3D kinematic assessment. Knee Surg. Sport. Traumatol. Arthrosc. 23, 3259–3265. https://doi.org/10.1007/s00167-014-3169-0.
Shanbehzadeh, S., Mohseni Bandpei, M.A., Ehsani, F., 2017. Knee muscle activity during gait in patients with anterior cruciate ligament injury: a systematic review of electromyographic studies. Knee Surg. Sport. Traumatol. Arthrosc. 25, 1432–1442. https://doi.org/10.1007/s00167-015-3925-9.
Shao, Q., MacLeod, T.D., Manal, K., Buchanan, T.S., 2011. Estimation of ligament loading and anterior tibial translation in healthy and ACL-deficient knees during gait and the influence of increasing tibial slope using EMG-driven approach. Ann. Biomed. Eng. 39, 110–121. https://doi.org/10.1007/s10439-010-0131-2.
Sharifi, M., Shirazi-Adl, A., Marouane, H., 2017. Computational stability of human knee joint at early stance in Gait: effects of muscle coactivity and anterior cruciate ligament deficiency. J. Biomech. 63, 110–116. https://doi.org/10.1016/j.jbiomech.2017.08.004.
Shelburne, K.B., Pandy, M.G., Torry, M.R., 2004. Comparison of shear forces and ligament loading in the healthy and ACL-deficient knee during gait. J. Biomech. 37, 313–319. https://doi.org/10.1016/j.jbiomech.2003.07.001.
Shelburne, K.B., Torry, M.R., Pandy, M.G., 2005. Effect of muscle compensation on knee instability during ACL-deficient gait. Med. Sci. Sports Exerc. 37, 642–648. https://doi.org/10.1249/01.MSS.0000158187.79100.48.
Shelburne, K.B., Torry, M.R., Yanagawa, T., Pandy, M.G., 2003. Theoretical analysis of the flexed knee pattern in ACL-deficient gait. Summer Bioengineering Conference.
Smith, C.R., Lenhart, R.L., Kaiser, J., Vignos, M.F., Thelen, D.G., 2015. Influence of ligament properties on tibiofemoral mechanics in walking. J. Knee Surg. https://doi.org/10.1055/s-0035-1558858.
Smith, R.C., Choi, K.W., Negrut, D., Thelen, D.G., 2016. Efficient computation of cartilage contact pressures within dynamic simulations of movement. Comput. Methods Biomech. Biomed. Eng. Imaging Vis., 1163 https://doi.org/10.1080/21681163.2016.1172346.
Spang, J.T., Dang, A.B.C., Mazzocca, A., Rincon, L., Obopilwe, E., Beynnon, B., Arciero, R.A., 2010. The effect of medial meniscectomy and meniscal allograft transplantation on knee and anterior cruciate ligament biomechanics. Arthrosc. – J. Arthrosc. Relat. Surg. 26, 192–201. https://doi.org/10.1016/j.arthro.2009.11.008.
Steele, K.M., DeMers, M.S., Schwartz, M.H., Delp, S.L., 2012. Compressive tibiofemoral force during crouch gait. Gait Posture 35, 556–560. https://doi.org/10.1016/j.gaitpost.2011.11.023.
Stergiou, N., Ristanis, S., Moraiti, C., Georgoulis, A.D., 2007. Tibial rotation in anterior cruciate ligament (ACL) – deficient and ACL-reconstructed knees. Sport. Med 37, 601–613. https://doi.org/10.2165/00007256-200737070-00004.
Torry, M.R., Decker, M.J., Ellis, H.B., Shelburne, K.B., Sterett, W.I., Steadman, J.R., 2004. Mechanisms of compensating for anterior cruciate ligament deficiency during gait. Med. Sci. Sports Exerc. 36, 1403–1412. https://doi.org/10.1249/01.MSS.0000135797.09291.71.
Trojani, C., Sbihi, A., Djian, P., Potel, J.F., Hulet, C., Jouve, F., Bussière, C., Ehkirch, F.P., Burdin, G., Dubrana, F., Beaufils, P., Franceschi, J.P., Chassaing, V., Colombet, P., Neyret, P., 2011. Causes for failure of ACL reconstruction and influence of meniscectomies after revision. Knee Surg. Sport. Traumatol. Arthrosc. 19, 196–201. https://doi.org/10.1007/s00167-010-1201-6.
Victor, J., Labey, L., Wong, P., Innocenti, B., Bellemans, J., 2010. The influence of muscle load on tibiofemoral knee kinematics. J. Orthop. Res. 28, 419–428. https://doi.org/10.1002/jor.21019.
Waite, J.C., Beard, D.J., Dodd, C.A.F., Murray, D.W., Gill, H.S., 2005. In vivo kinematics of the ACL-deficient limb during running and cutting. Knee Surg. Sport. Traumatol. Arthrosc. 13, 377–384. https://doi.org/10.1007/s00167-004-0569-6.
Wexler, G., Hurwitz, D.E., Bush-Joseph, C.A., Andriacchi, T.P., Bach Jr., B.R., 1998. Functional gait adaptations in patients with anterior cruciate ligament deficiency over time. Clin. Orthop. Relat. Res. 166–175. https://doi.org/10.1556/AAlim. 2015.0002.
Yanagawa, T., Shelburne, K., Serpas, F., Pandy, M., 2002. Effect of hamstrings muscle action on stability of the ACL-deficient knee in isokinetic extension exercise. Clin. Biomech. 17, 705–712. https://doi.org/10.1016/S0268-0033(02)00104-3.